Supplemental Materials

Soil textures rather than root hairs dominate water uptake and soil-plant hydraulics under drought

Gaochao Cai[1, 2], Andrea Carminati[3], Mohanned Abdalla[1], and Mutez Ali Ahmed[1, 2*]

[1]Chair of Soil Physics, Bayreuth Center of Ecology and Environmental Research (BayCEER), University of Bayreuth, Universitätsstraße 30, 95447, Bayreuth, Germany

[2]Biogeochemistry of Agroecosystems, University of Göttingen, Büsgenweg 2, 37077, Göttingen, Germany

[3]Physics of Soils and Terrestrial Ecosystems, Institute of Terrestrial Ecosystems, Department of Environmental Systems Science, ETH Zürich, Universitätstr. 16, 8092, Zurich, Switzerland

[*]Corresponding author: Mutez Ali Ahmed

Email: Mutez.Ahmed@uni-bayreuth.de

Supplemental Figures

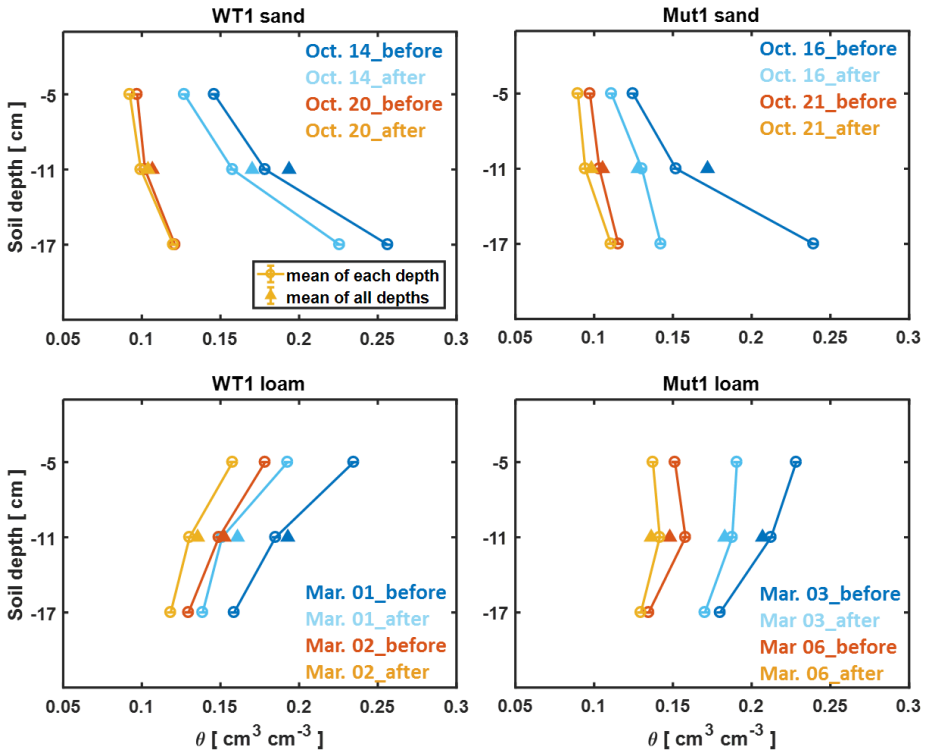

Supplemental Figure S1. Example of soil water content (θ) distribution at three locations along the soil column for a wild type (WT) and mutant (Mut) before and after the root pressure chamber measurements. n = 3 at each depth.

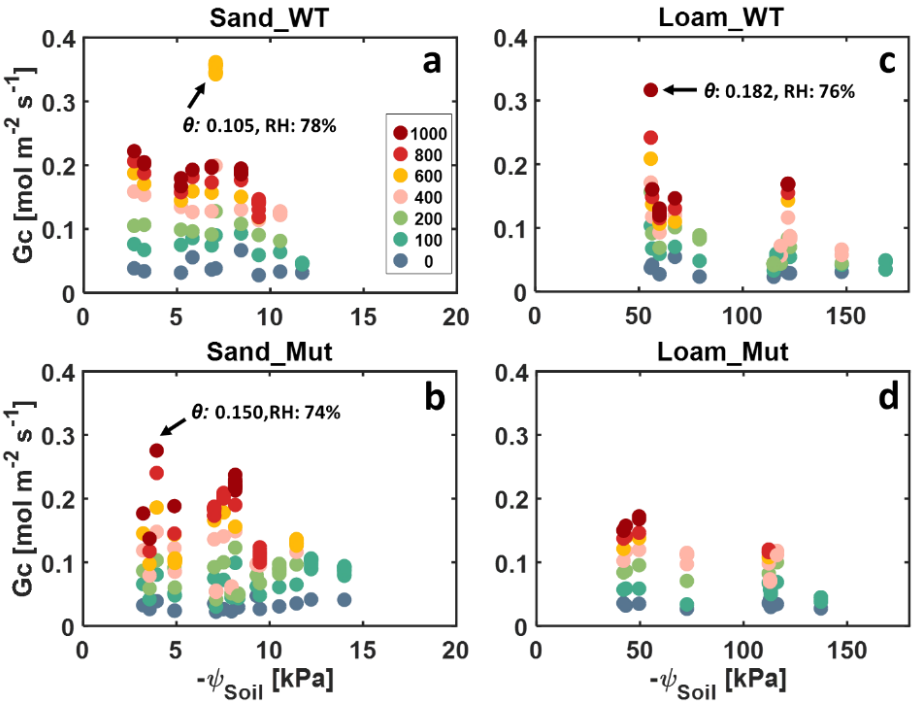

Supplemental Figure S2. Canopy stomatal conductance (*Gc*) of wild-type (WT) and mutant (Mut) in sand and loam at different light intensities (μmol m^{-2} s^{-1}) during soil drying. (**a**-**b**) sand and (**c**-**d**) loam. The legend in (**a**) is for the light intensity**.** Arrows showed exceptions with higher relative humidity (RH) of the outgoing air due to moist air in the laboratory, which results in a lower vapor pressure deficit (*VPD*). More than two points of the same color at one soil matric potential (ψ_{Soil}) mean that the applied pressure could not be sustained at that light intensity. Eliminating three exceptions with higher relative humidity (causing lower *VPD*), effects of individual factors and interactions between different factors on canopy conductance were also similar to E_{norm} (Supplemental Table S2).

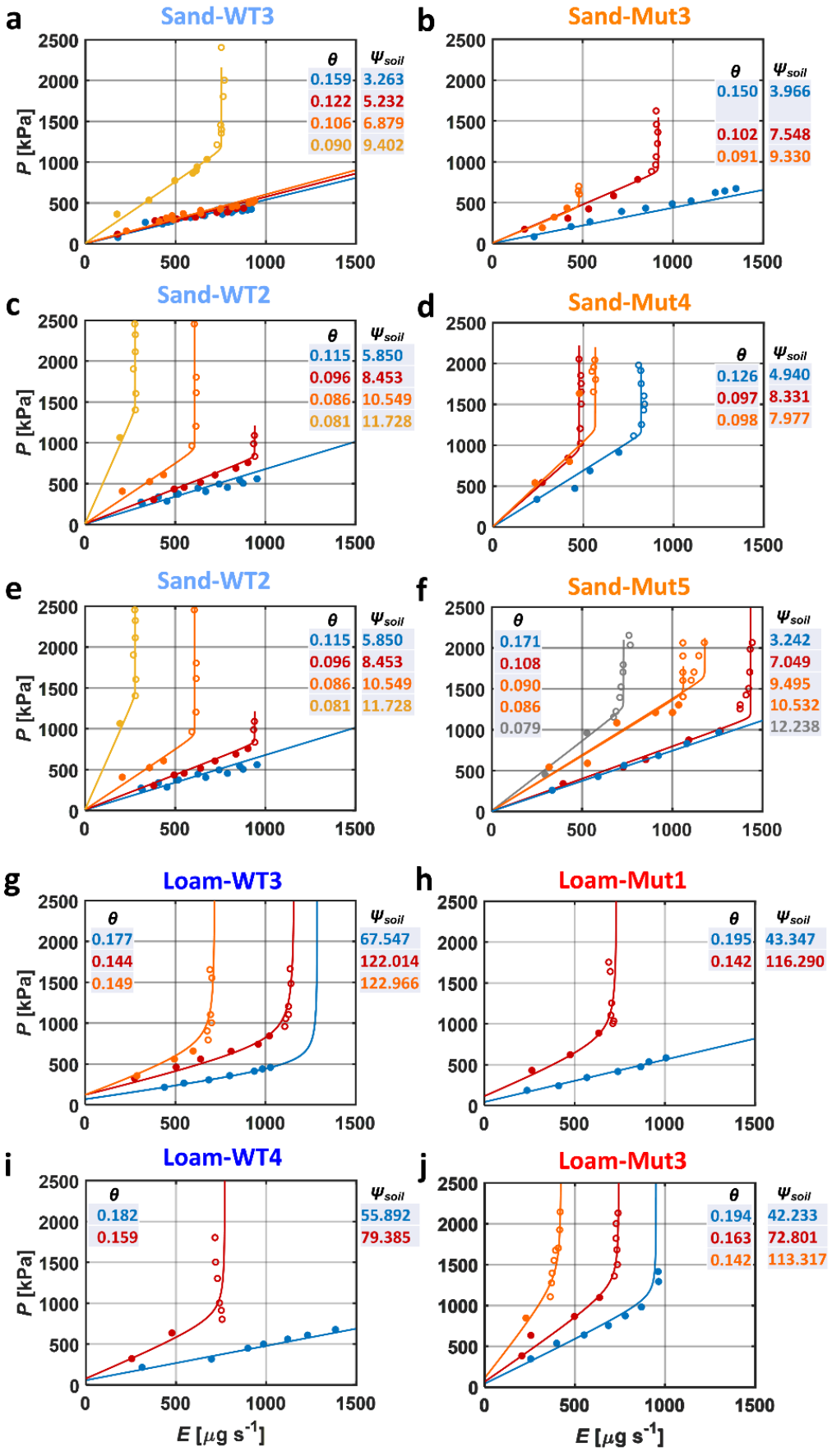
a
Sand-WT3
b
Sand-Mut3
c
Sand-WT2
d
Sand-Mut4
e
Sand-WT2
f
Sand-Mut5
g
Loam-WT3
h
Loam-Mut1
i
Loam-WT4
j
Loam-Mut3
P [kPa]
E [μg s-1]
θ
Ψsoil
0.159 3.263
0.122 5.232
0.106 6.879
0.090 9.402
0.150 3.966
0.102 7.548
0.091 9.330
0.115 5.850
0.096 8.453
0.086 10.549
0.081 11.728
0.126 4.940
0.097 8.331
0.098 7.977
0.171 3.242
0.108 7.049
0.090 9.495
0.086 10.532
0.079 12.238
0.177 67.547
0.144 122.014
0.149 122.966
0.195 43.347
0.142 116.290
0.182 55.892
0.159 79.385
0.194 42.233
0.163 72.801
0.142 113.317

Supplemental Figure S3. Relation between balancing pressure (P, $-\psi_{leaf\_x}$) and transpiration rate (E) in wild-type (WT) and mutant (Mut) in sand and loam during soil drying. (**a-f**) sand. (**g-j**) loam. Close symbols are the measurements with steady-state balancing pressure whereas open symbols are recorded pressure when no steady-state could be reached. Same color was used for the curves and corresponding soil water content (θ, $cm^3\ cm^{-3}$) and soil matric potential (ψ_{Soil}, kPa) (values next to the curves). ψ_{Soil} was averaged from individual soil water content along the soil column. 'Sand-WT2' in (**c** and **e**) was the same plant as that in **Fig. 5c**. 'Loam-Mut1' in (**h**) was the same plant as that in **Fig. 5f**. Repeated usage of the same plants was to make a better comparison between genotypes.

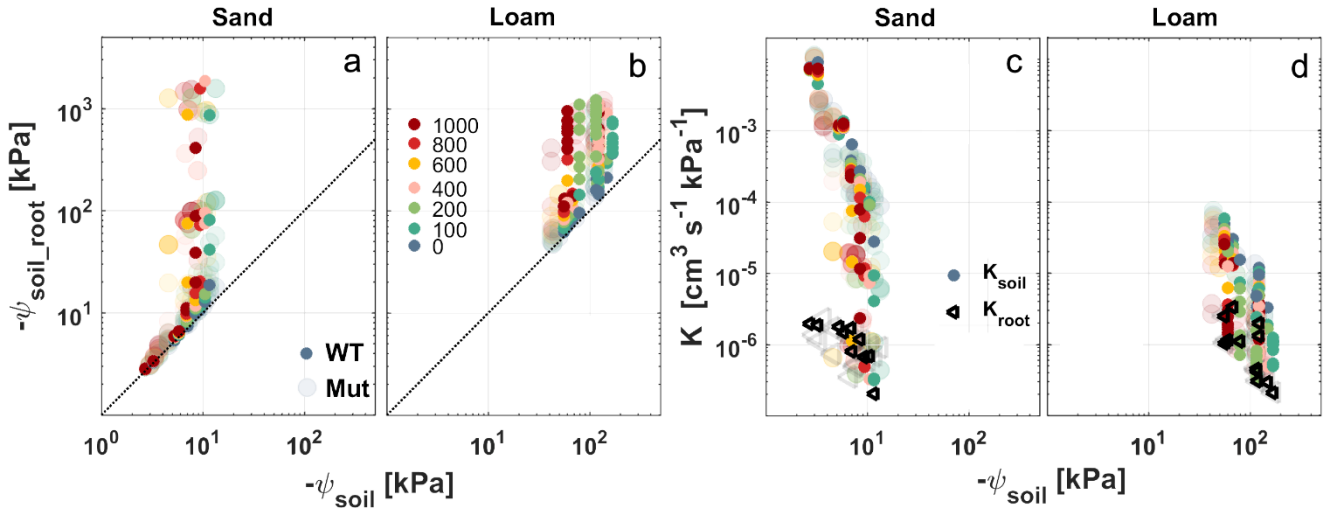

Supplemental Figure S4. Comparison between matric potential at the soil-root interface (ψ_{soil_root}) and in the bulk soil (ψ_{Soil}) and comparison between soil conductance (K_{soil}) and root hydraulic conductance (K_{root}) for the wild-type (WT) and mutant (Mut) grown in sand and loam. Variations of matric potential and conductance with increasing transpiration rate were presented by the color of light intensity steps from blue-green to red (the legend in the second subplot, µmol $m^{-2}\ s^{-1}$). Note that (**a-b**) were from **Fig. 6** while (**c-d**) were from **Fig. 7**.

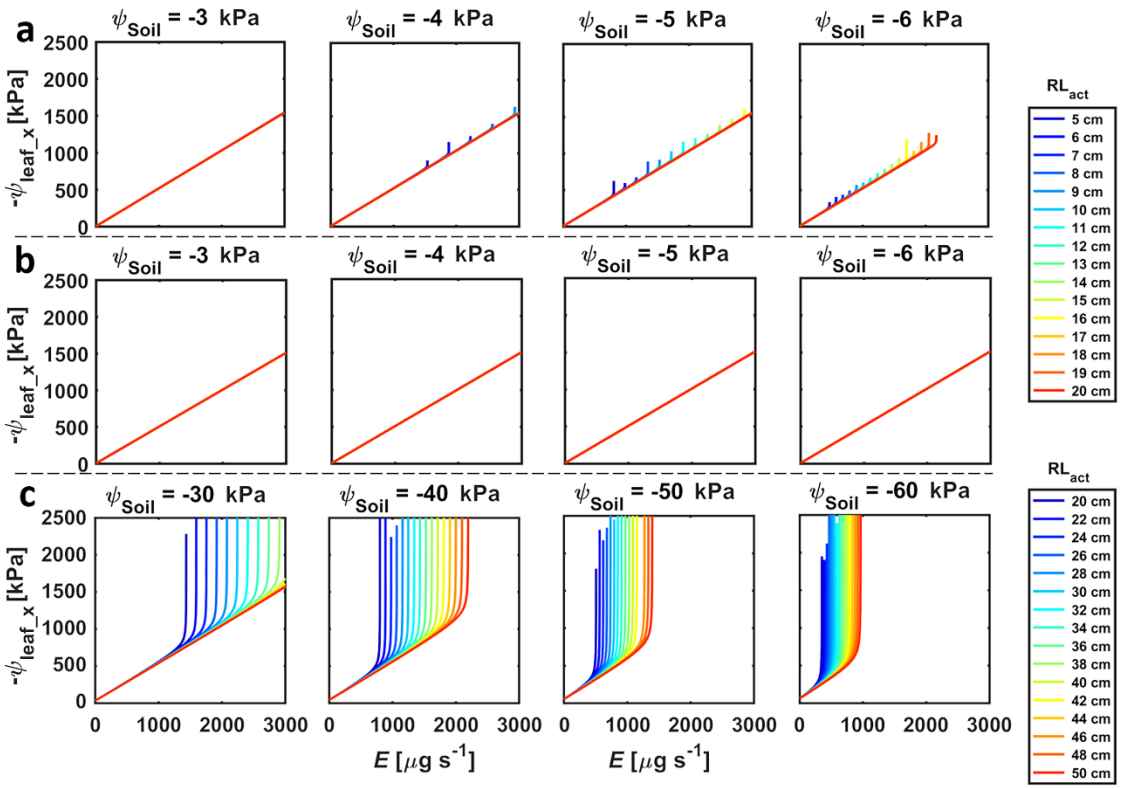

Supplemental Figure S5. Sensitivity analysis of active root length (RL_{act}) on leaf xylem water potential (ψ_{leaf_x}) for different soil matric potentials (ψ_{Soil}) in sand and loam. (**a**) sand. (**b-c**) loam. After curve bending, the less negative ψ_{leaf_x} in sand than in loam was due to using the same resolution of E (1 µg s^{-1}) for all simulations.

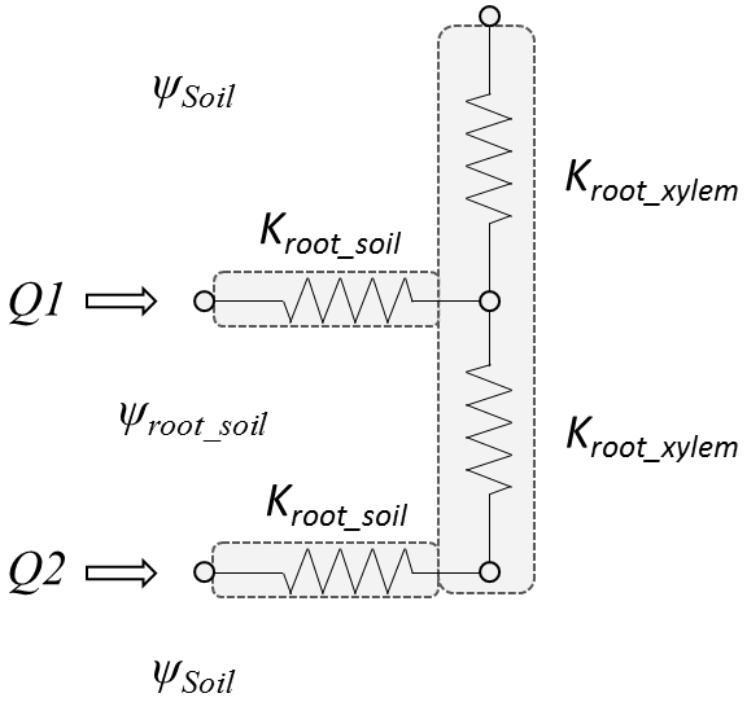

Supplemental Figure S6. Scheme of the simple root hydraulic architecture model of water uptake. K_{root_xylem}: root xylem hydraulic conductance (kPa cm^{-3} s), K_{roor_soil}: hydraulic conductance at the soil-root interface (kPa cm^{-3} s), ψ_{Soil}: soil matric potential (kPa), ψ_{root_soil}: matric potential at the soil-root interface (kPa), Q1: water uptake in the first layer ($cm^3\ s^{-1}$), Q2: water uptake in the second layer ($cm^3\ s^{-1}$).

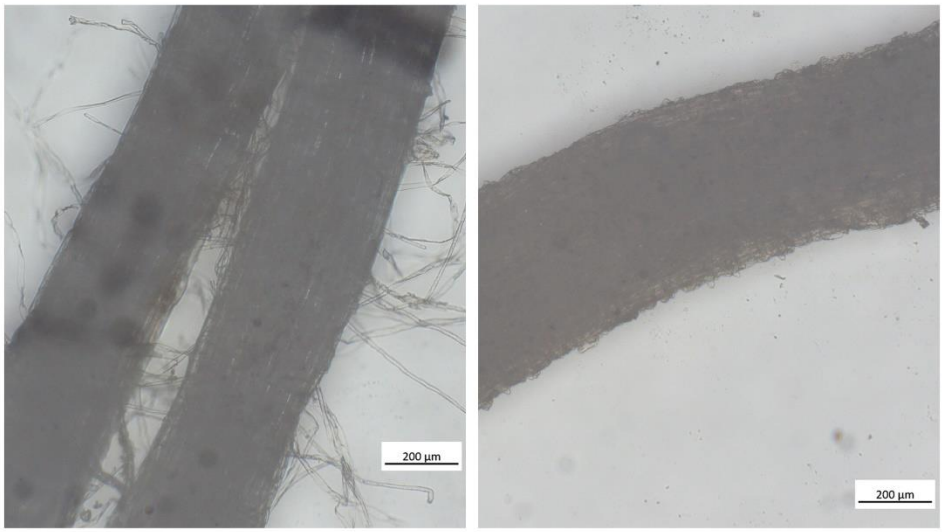

Supplemental Figure S7. Images of wild-type and mutant roots from plants grown in sand. Left: wild-type, right: mutant. The images were captured using a reflected light microscope (Axio Imager 2, Carl Zeiss) equipped with a digital camera (Axiocam 305, software Zen 2 cores, Carl Zeiss). Root samples were from lateral roots (ca. 5 cm above root tips) of the plants at 36 days after sowing when all measurements of transpiration rate and leaf xylem water potential were finished.

Supplemental Tables

Supplemental Table S1. Analysis of variance (ANOVA) considering three-way interaction for the influence of different factors on normalized transpiration rate (E_{norm}) shown in Figure 4.

Source	SS[¶]	DF	MS	F	Prob>F
Soil type	2.57e-12	1	2.57e-12	14.84	0.0002***
Genotype	1.33e-14	1	1.33e-14	0.08	0.7826
Soil matric potential [¶¶]	1.95e-13	2	9.75e-14	0.57	0.5692
Light intensity	1.53e-10	6	2.56e-11	146.74	<0.001***
Replicate (Soil type, Genotype, Soil matric potential, Light intensity)	1.89e-11	104	1.82e-13	1.98	0.0014**
Soil type * Genotype	2.50e-15	1	2.50e-15	0.01	0.9045
Soil type * Soil matric potential	5.06e-14	2	2.53e-14	0.15	0.8645
Soil type * Light intensity	9.50e-13	6	1.58e-13	0.9	0.4973
Genotype * Soil matric potential	2.13e-14	2	1.06e-14	0.06	0.9409
Genotype * Light intensity	4.87e-13	6	8.12e-14	0.46	0.8385
Soil matric potential * Light intensity	1.54e-12	12	1.29e-13	0.73	0.7152
Soil type * Genotype * Soil matric potential	3.31e-15	2	1.66e-15	0.01	0.9907
Soil type * Genotype * Light intensity	9.71e-13	6	1.62e-13	0.93	0.4783
Genotype * Soil matric potential * Light intensity	1.45e-12	12	1.21e-13	0.68	0.7689
Soil type * Soil matric potential * Light intensity	2.85e-12	12	2.37e-13	1.35	0.2001
Error	6.34e-12	69	9.18e-14		
Total	2.60e-10	244			

[¶]SS: sum of squares, DF: degree of freedom, MS: mean sum of squares, F: F-statistic value. p<0.001***, p<0.01**, p<0.05*.

[¶¶] Soil matric potential in both soils was normalized to be in the range of 0 and 1. Group 1, 2, and 3 for each genotype was from 0 to 0.2 (wet soil), 0.2 to 0.6 (moderate dry), and 0.6 to 1 (dry) where all the $P(E)$ curves were linear (bent at high water content), either linear or nonlinear, and nonlinear, respectively. This ensures at least two $P(E)$ measurements in each group from each genotype and soil type.

Supplemental Table S2. Analysis of variance (ANOVA) considering three-way interaction for the influence of different factors on canopy stomatal conductance (*Gc*) shown in Supplemental Figure S2.

Source	SS[¶]	DF	MS	F	Prob>F
Soil type	1.49e-02	1	1.49e-02	24.35	<0.001***
Genotype	1.73e-03	1	1.73e-03	2.84	0.0950
Soil matric potential[¶¶]	2.80e-04	2	1.40e-04	0.23	0.7929
Light intensity	3.31e-01	6	5.52e-02	90.13	<0.001***
Replicate (Soil type, Genotype, Soil matric potential, Light intensity)	6.40e-02	98	6.50e-04	2.96	<0.001***
Soil type * Genotype	1.46e-03	1	1.46e-03	2.4	0.1245
Soil type * Soil matric potential	6.10e-04	2	3.00e-04	0.5	0.6088
Soil type * Light intensity	4.68e-03	6	7.80e-04	1.25	0.2850
Genotype * Soil matric potential	7.70e-04	2	3.80e-04	0.63	0.5361
Genotype * Light intensity	1.40e-04	6	2.00e-05	0.04	0.9998
Soil matric potential * Light intensity	3.91e-03	12	3.30e-04	0.53	0.8913
Soil type * Genotype * Soil matric potential	6.00e-05	2	3.00e-05	0.05	0.9546
Soil type * Genotype * Light intensity	2.73e-03	6	4.50e-04	0.74	0.6193
Genotype * Soil matric potential * Light intensity	3.73e-03	12	3.10e-04	0.49	0.9145
Soil type * Soil matric potential * Light intensity	1.01e-02	12	8.40e-04	1.35	0.2009
Error	1.48e-02	67	2.20e-04		
Total	6.52e-01	236			

[¶]SS: sum of squares, DF: degree of freedom, MS: mean sum of squares, F: F-statistic value. $p <$ 0.001***, $p < 0.01$**, $p < 0.05$*.

[¶¶] Soil matric potential in both soils was normalized to be in the range of 0 and 1. Group 1, 2, and 3 for each genotype was from 0 to 0.2 (wet soil), 0.2 to 0.6 (moderate dry), and 0.6 to 1 (dry) where all the $P(E)$ curves were linear (bent at high water content), either linear or nonlinear, and nonlinear, respectively. This ensures at least two $P(E)$ measurements in each group from each genotype and soil type. Exceptions with high relative humidity in Supplemental Figure S2 were not considered in this analysis.

Supplemental Table S3. Analysis of covariance (ANCOVA) for the regression slopes of relation between soil (ψ_{Soil}) and root hydraulic (K_{root} and RL_{act}) parameters for genotypes and soil types shown in Figure 7.

Parameters (in subplot of Fig. 7)	Soil type (p)	Genotype (p)	ψ_{Soil} or K_s (p)	Interaction between Soil/Geno- types and ψ_{Soil} or K_s (p)
ψ_{soil} vs K_{root} of WT and Mut in Sand (a)	-	0.9695	0.0011**	0.1202
ψ_{soil} vs K_{root} of WT and Mut in Loam (a)	-	0.2838	0.001***	0.2176
ψ_{soil} vs K_{root} in sand and loam (a)	< 0.001***	-	< 0.001***	0.2891
ψ_{soil} vs RL_{act} of WT and Mut in Sand (b)	-	0.3082	< 0.001***	0.0960
ψ_{soil} vs RL_{act} of WT and Mut in Loam (b)	-	0.6845	< 0.001***	0.2220
ψ_{soil} vs RL_{act} in sand and loam (b)	0.0115*	-	< 0.001***	0.6411
ψ_{soil} vs RL_{act} / RL_{total} in sand and loam (c)	0.6661	-	0.0008***	0.9656

$p < 0.001$***, $p < 0.01$**, $p < 0.05$*.

Supplemental Table S4. Fertilizer applied to the sandy and loamy soils.

Soil	Nutrient	Application rate (mg kg^{-1} soil)	Type
Sand	N	20	NH_4NO_3
	P	80	$CaHPO_4$
	K	20	K_2SO_4
	Mg	10	$MgCl_2 \times 6H_2O$
	Ca	100	$CaSO_4 \times 2H_2O$
	Mn	0.65	$MnSO_4 \times H_2O$
	Zn	0.16	$Zn(NO_3)_2 \times 4H_2O$
	Cu	0.10	$CuSO_4 \times 5H_2O$
	B	0.03	H_3BO_3
	Fe	0.65	Fe-EDTA
Loam	N	10	NH_4NO_3
	P	40	$CaHPO_4$
	K	10	K_2SO_4
	Mg	5	$MgCl_2 \times 6H_2O$

Supplemental Method S1: extended description of the soil-plant hydraulic model

The water flow from soil into roots is described by the Richards equation:

$$\frac{\partial \theta}{\partial t} = \frac{1}{r}\frac{\partial}{\partial r}\left(r k_s(h)\frac{\partial h}{\partial r}\right) \qquad \text{(Eq. S1)}$$

where θ is the volumetric water content ($cm^3\ cm^{-3}$), t is time (s), r is the radial coordinate (cm), k_s is the soil hydraulic conductivity ($cm\ s^{-1}$), and h is the water matric head (cm), which is the quotient of soil matric potential by the product of gravity g and water density ρ ($h = \psi_{Soil}/\rho g$).

We assumed a steady-rate behavior for the water flow in soil. Eq. S1 can be linearized to matric flux potential (Φ, $cm^2\ s^{-1}$) as the integral of hydraulic conductivity (k) over matric head using the Kirchhoff transformation approach (de Jong van Lier et al., 2008):

$$\Phi(\psi) = \int_{-\infty}^{\psi} k(x)dx \qquad \text{(Eq. S2)}$$

The flux boundary condition at the soil-root interface was obtained by combining the radial Richards equation S1, S2 and Eq. 2 (Schröder et al., 2009):

$$\Phi_{soil\_root} = -\frac{E}{2\pi\, RL_{act}}\left(\frac{1}{2} - r_b^2\frac{ln(r_b/r_0)}{r_b^2 - {r_0}^2}\right) + \Phi_{Soil} \qquad \text{(Eq. S3)}$$

where Φ_{soil_root} and Φ_{Soil} are the matric flux potentials ($cm^2\ s^{-1}$) at the soil-root interface and the bulk soil, respectively. E is the transpiration rate ($cm^3\ s^{-1}$). RL_{act} is the active root length (cm), and r_0 and r_b are root and rhizosphere radius (cm), respectively. Φ_{Soil} can be calculated using Eq.S2 and 3. Consequently, the matric potential at the soil-root interface ψ_{soil_root} can be obtained based on Eq S2, S3, and 3:

$$\psi_{soil\_root} = \left(\frac{\frac{\psi_0^{\tau}\,\psi_{Soil}^{1-\tau}\,k_{sat}}{\tau - 1} - \Phi_{Soil}}{\frac{\psi_0^{\tau}\,k_{sat}}{\tau - 1}}\right)^{\frac{1}{1-\tau}} \qquad \text{(Eq. S4)}$$

where ψ_0 and τ are parameters in the Brooks and Corey model described in Eq. 3, and k_{sat} is the saturated soil hydraulic conductivity ($cm\ s^{-1}$) in Eq. 3.

The water flow in the xylem is described by:

$$E = K_x(\psi_{xylem\_root} - \psi_{leaf\_x}) \qquad \text{(Eq. S5)}$$

where K_x is the aboveground xylem conductance ($cm^3\ kPa^{-1}\ s^{-1}$), and is derived from the root hydraulic conductance (K_{root}):

$$K_x(\psi) = K_{root}\left(\frac{\psi_{Soil}}{\psi_{xylem\_0}}\right)^{-\tau_x} \qquad \text{(Eq. S6)}$$

where ψ_{xylem_0} is the matric potential when the xylem cavitates (kPa). In this study, we pressurized the plants and xylem cavitation is excluded. A value negative than 1500 kPa was used in the model, i.e., -3000 kPa. τ_x is a constant (-), and 5 is used in this study. Therefore, $K_x >> K_{root}$.

The hydraulic conductance of a whole plant (K_{plant}) is composed of K_x and K_{root}:

$$\frac{1}{K_{plant}} = \frac{1}{K_{root}} + \frac{1}{K_x} \qquad \text{(Eq. S7)}$$

K_{plant} is approximately equal to K_{root} in this study when combing Eq. S6 and Eq. S7.

Flux matric potential could also be used to link the flow between leaf and xylem according to Eq S2:

$$\Phi_{leaf\_x} = -E + \Phi_{xylem\_root} \qquad \text{(Eq. S8)}$$

from which ψ_{leaf_x} can be derived when combing Eq. S4, S5, S6, and 5.

$$\psi_{leaf\_x} = \left(\psi_{xylem\_root}^{1-\tau_x} - \frac{E\,(\tau_x - 1)}{\psi_{xylem\_0}^{\tau_x}\ K_{root}}\right)^{\frac{1}{1-\tau_x}} \qquad \text{(Eq. S9)}$$

Supplemental references:

de Jong van Lier Q, van Dam JC, Metselaar K, de Jong R, Duijnisveld WHM (2008) Macroscopic Root Water Uptake Distribution Using a Matric Flux Potential Approach. Vadose Zone Journal **7**: 1065

Schröder T, Javaux M, Vanderborght J, Körfgen B, Vereecken H (2009) Implementation of a Microscopic Soil–Root Hydraulic Conductivity Drop Function in a Three-Dimensional Soil–Root Architecture Water Transfer ModelAll rights reserved. Vadose Zone Journal **8**: 783–792